

Characterization of energy transfer for passively Q-switched laser ignition

S. Lorenz,^{*} M. Bärwinkel, P. Heinz, S. Lehmann, W. Mühlbauer and D. Brüggemann

University of Bayreuth, Chair of Engineering Thermodynamics and Transport Processes, Universitätsstraße 30,
95447 Bayreuth, Germany
^{*}litt@uni-bayreuth.de

Abstract: Miniaturized passively Q-switched Nd:YAG/Cr⁴⁺:YAG lasers are promising candidates as spark sources for sophisticated laser ignition. The influence of the complex spatial-temporal pulse profile of such lasers on the process of plasma breakdown and on the energy transfer is studied. The developed measurement technique is applied to an open ignition system as well as to prototypes of laser spark plugs. A detected temporal breakdown delay causes an advantageous separation of plasma building phase from energy transfer. In case of fast rising laser pulses, an advantageous reduction of the plasma breakdown delay occurs instead.

©2015 Optical Society of America

OCIS codes: (140.0140) Lasers and laser optics; (140.3440) Laser-induced breakdown; (140.3540) Lasers, Q-switched; (140.3295) Laser beam characterization; (260.2160) Energy transfer.

References and links

1. D. Bradley, C. Sheppard, I. Suardjaja, and R. Woolley, "Fundamentals of high-energy spark ignition with lasers," *Combust. Flame* **138**(1-2), 55–77 (2004).
2. T. X. Phuoc, "Laser-induced spark ignition fundamental and applications," *Opt. Lasers Eng.* **44**(5), 351–397 (2006).
3. M. H. Morsy, "Review and recent developments of laser ignition for internal combustion engines applications," *Renew. Sustain. Energy Rev.* **16**(7), 4849–4875 (2012).
4. J. Tauer, H. Kofler, and E. Wintner, "Laser-initiated ignition," *Laser Photon. Rev.* **4**(1), 99–122 (2010).
5. S. B. Gupta, B. Munidhar, B. Bipin, and S. Raj, "Natural Gas Fired Reciprocating Engines for Power Generation: Concerns and Recent Advances," in *Natural Gas - Extraction to End Use*, S. Gupta, ed. (InTech, 2012).
6. M. Weinrotter, H. Kopecek, M. Tesch, E. Wintner, M. Lackner, and F. Winter, "Laser ignition of ultra-lean methane/hydrogen/air mixtures at high temperature and pressure," *Exp. Therm. Fluid Sci.* **29**(5), 569–577 (2005).
7. D. Böker and D. Brüggemann, "Advancing lean combustion of hydrogen-air mixtures by laser-induced spark ignition," *Int. J. Hydrogen Energy* **36**(22), 14759–14767 (2011).
8. D. Böker and D. Brüggemann, "Temperature measurements in a decaying laser-induced plasma in air at elevated pressures," *Spectrochim. Acta, B At. Spectrosc.* **66**(1), 28–38 (2011).
9. E. Schwarz, S. Gross, B. Fischer, I. Muri, J. Tauer, H. Kofler, and E. Wintner, "Laser-induced optical breakdown applied for laser spark ignition," *Laser Part. Beams* **28**(01), 109 (2010).
10. D. K. Srivastava, E. Wintner, and A. K. Agarwal, "Effect of focal size on the laser ignition of compressed natural gas-air mixture," *Opt. Lasers Eng.* **58**, 67–79 (2014).
11. J. D. Mullett, R. Dodd, C. J. Williams, G. Triantos, G. Dearden, A. T. Shenton, K. G. Watkins, S. D. Carroll, A. D. Scarisbrick, and S. Keen, "The influence of beam energy, mode and focal length on the control of laser ignition in an internal combustion engine," *J. Phys. D Appl. Phys.* **40**(15), 4730–4739 (2007).
12. T. X. Phuoc, "Laser spark ignition: experimental determination of laser-induced breakdown thresholds of combustion gases," *Opt. Commun.* **175**(4-6), 419–423 (2000).
13. M. Weinrotter, B. Schwecherl, H. Kopecek, E. Wintner, J. Klausner, and G. Herdin, "Laser-Ignition of Methane-Air Mixtures at High Pressures and Temperatures European Combustion Meeting (2005).
14. J. K. Koga, K. Moribayashi, Y. Fukuda, S. V. Bulanov, A. Sagisaka, K. Ogura, H. Daido, M. Yamagiwa, T. Kimura, T. Fujikawa, M. Ebina, and K. Akihama, "Simulation and experiments of the laser induced breakdown of air for femtosecond to nanosecond order pulses," *J. Phys. D Appl. Phys.* **43**(2), 025204 (2010).
15. M. J. Myers, J. D. Myers, B. Guo, C. Yang, C. R. Hardy, J. J. Thomas, and F. M. Dickey, "Practical internal combustion engine laser spark plug development," in *Photonic Devices + Applications*, SPIE Proceedings (SPIE, 2007), pp. 66620E.

16. G. Herdin, J. Klausner, E. Wintner, M. Weinrotter, J. Graf, and K. Iskra, "Laser Ignition - a New Concept to Use and Increase the Potentials of Gas Engines," in *ARES-ARICE Symposium on Gas Fired Reciprocating Engines*, ICEF2005–1352.
17. G. Kroupa, F. Georg, and W. Ernst, "Novel miniaturized high-energy Nd-YAG laser for spark ignition in internal combustion engines," *Opt. Eng.* **48**(1), 014202 (2009).
18. J. Schwarz, P. Wörner, K. Stoppel, K.-H. Nübel, and J. Engelhardt, "Pumping concepts for laser spark plugs - Requirements, options, solutions," presented at 2nd Laser Ignition Conference, Yokohama, Japan, 21–24 Apr. 2014.
19. T. Dascalu, G. Salamu, O. Sandu, M. Dinca, and N. Pavel, "Scaling and passively Q-switch operation of a Nd:YAG laser pumped laterally through a YAG prism," *Opt. Laser Technol.* **67**, 164–168 (2015).
20. N. Pavel, M. Tsunekane, and T. Taira, "Composite, all-ceramics, high-peak power Nd:YAG/Cr(4+):YAG monolithic micro-laser with multiple-beam output for engine ignition," *Opt. Express* **19**(10), 9378–9384 (2011).
21. M. Tsunekane, T. Inohara, A. Ando, N. Kido, K. Kanephara, and T. Taira, "High Peak Power, Passively Q-switched Microlaser for Ignition of Engines," *IEEE J. Quantum Electron.* **46**(2), 277–284 (2010).
22. H. Moench and G. Derra, "High Power VCSEL Systems," *Laser Technik J.* **11**(2), 43–47 (2014).
23. M. Tsunekane and T. Taira, "Compact and Wide Temperature Acceptance of VCSEL-pumped Micro-Laser for Laser Ignition," in *Advanced Solid State Lasers*, pp. ATu3A.58.
24. J. Zabkar, M. Marincek, and M. Zgonik, "Mode Competition During the Pulse Formation in Passively Q-switched Nd:YAG Lasers," *IEEE J. Quantum Electron.* **44**(4), 312–318 (2008).
25. L. J. Radziemski and D. A. Cremers, "Laser-induced plasmas and applications" (M. Dekker, ©1989).
26. T. X. Phuoc and F. P. White, "Laser-induced spark ignition of CH₄/air mixtures," *Combust. Flame* **119**(3), 203–216 (1999).
27. E. Yablonovitch, "Self-phase modulation and short-pulse generation from laser-breakdown plasmas," *Phys. Rev. A* **10**(5), 1888–1895 (1974).
28. H. Kopecek, H. Maier, G. Reider, F. Winter, and E. Wintner, "Laser ignition of methane-air mixtures at high pressures," *Exp. Therm. Fluid Sci.* **27**(4), 499–503 (2003).
29. M. Weinrotter, H. Kopecek, E. Wintner, M. Lackner, and F. Winter, "Application of laser ignition to hydrogen-air mixtures at high pressures," *Int. J. Hydrogen Energy* **30**(3), 319–326 (2005).
30. Y.-L. Chen, J. Lewis, and C. Parigger, "Spatial and temporal profiles of pulsed laser-induced air plasma emissions," *J. Quant. Spectrosc. Radiat. Transf.* **67**(2), 91–103 (2000).

1. Introduction

Ongoing further developments in engine combustion are driven by the aim to reduce fuel consumption and emissions. Two concepts pursued by engine developers are leaner burning and downsizing. Both approaches lead to increasing challenges concerning ignition as these concepts are typically associated with an increase in the flow velocity and the degree of turbulence as well as higher pressure at the time of ignition. In this context, laser ignition can be regarded as a very promising alternative. Many advantages of laser ignition have been investigated yet under laboratory conditions [1–4]. Beside a lower energy demand at increasing brake mean effective pressures, the lower ignition limit for lean mixtures has to be emphasized [5–7].

The non-resonant laser-induced breakdown process can be described in four steps: A focused laser pulse causes an electron cascade process at a sufficient level of laser irradiance. Subsequently, an expanding high-temperature and high-pressure plasma is generated. The expansion ends after 0.5 – 2 µs by emitting a shockwave [8]. After another 10 – 50 µs a self-sustaining chain branch of chemical reactions is built. This step takes place where local flow condition permits it and is associated with probability of flame kernel generation.

In this study, the energy transfer of a laser into the plasma is investigated as the first step of laser ignition processes. Most studies concerning the energy transfer and the plasma breakdown have been carried out with actively Q-switched nanosecond Nd:YAG lasers at fundamental or frequency-doubled wavelength. Schwarz et al. [9] show that 532 nm radiation is advantageous for generating a plasma breakdown because of tighter focus area, whereas 1064 nm radiation is advantageous for transferring more energy to the plasma due to a greater plasma absorption efficiency. Moreover, investigations show that increasing focal length leads to raised minimum energy for ignition (MIE) and lower power density [10,11]. By rising the ambient pressure, the MIE decreases. Due to different ionization energy levels, the breakdown limit depends on ambient gas [1,12]. Weinrotter et al. [13] detected in this context no significant difference between air and CH₄/air mixtures. In numerical simulations of the

laser induced breakdown in air, Koga et al. [14] show that the product of pulse duration and intensity has to be large enough for heating free electrons to energies of the order of 100 eV for occurring a large amount of ionization.

However, to offer a marketable alternative to conventional ignition systems, a laser spark plug has to meet additional requirements [15,16]: Laser and mount have to be resistant against shocks and vibrations and have to be operated in a wide range of temperatures. For application in current engine systems, the size of a laser spark plug has to be in the range of current spark plugs. Due to economic reasons, the total costs of ownership have to be acceptably low. Possible solutions to meet these requirements are miniaturized passively Q-switched lasers (PQL). The laser medium can be pumped by fiber-coupled diodes. Other pumping concepts are discussed by Kroupa et al. [17], Schwarz et al. [18] and Dascalu et al. [19]. A slight self-induced aperture effect of the saturable absorber results in high beam quality.

Due to tight setup, the size of a laser spark plug can be in the range of conventional spark plugs [20,21]. In the case of fiber-coupled pumping, the temperature sensitive diode laser can be separated from the engine. Moreover, temperature-insensitive pump sources and ceramic gain mediums are currently the subject of investigations [20,22,23]. However, in PQLs rising pump current and/or pump duration does not lead to more intensive single pulses, but causes a rising number of output pulses, each of them with nearly constant individual energy.

The energy transfer from laser pulse to plasma can be quantitatively analyzed by energy meters, as a customary method. Unfortunately, these detectors do not supply any information about temporal behavior of this transfer. Furthermore, their temporal resolving is too low to distinguish between individual pulses within a pulse interval. Therefore, highly resolved measurement techniques are in demand. Moreover, even in the case of good transversal mode quality, the transient aperture of partially saturated absorber causes a complex spatial transmission [24], shaping the laser pulse in the temporal and spatial regime. The impact of this pulse structure on plasma breakdown and energy transfer has not been studied systematically yet. For this, a reproducible method for analyzing the pulse shape is necessary providing temporal behavior of the pulse profile as well as the energy transfer and its amount of transferred energy. The method should be applicable for individual pulses of a pulse train. In addition, for the industrial application of PQL as spark plugs it is important that the energy transfer and the properties of the pulse profile can be analyzed at prototypes of laser spark plugs where the laser and the focusing unit are sealed in a mount.

The energy measurement techniques developed in this study distinguish between quantitative time-resolved measurements of global energy deposition and time-resolved measurements of local energy deposition, considering the energy distribution within the beam profile. The technique was applied firstly to an open PQL where the laser beam is focused by freestanding lenses to generate plasma. In a second step, the energy transfer of prototypes of laser spark plugs is investigated. At these plugs, the laser as well as the focusing elements and a window to the engine's combustion chamber are all sealed. This prevents sensing data directly within the device. New measurement strategies are required for detecting data like the energy distribution of the laser output.

The results of the local measurements support better understanding of the plasma breakdown process induced by PQL. Furthermore, the impact of a specific spatial and temporal energy distribution within the beam profiles of PQL is discussed.

2. Energy transfer of miniaturized passively Q-switched lasers

The gain crystal of the investigated PQL is end-pumped by a diode laser, resulting in a spatial radial symmetric pulse profile. The beam diameter in front of the focusing lens ($f = 8 \text{ mm}$) is about 8 mm. To achieve realistic engine-like conditions, the gain medium is heated up to 100 °C and the pump frequency is set to 12.5 Hz, corresponding to 1500 rpm. All PQLs are running in the fundamental wavelength of 1064 nm. Quantitative time-resolved

measurements of global energy deposition are discussed in chapter 2.1, while time-resolved measurements of local energy deposition, considering the energy distribution within the spatial beam profile are presented in chapter 2.2.

2.1 Global energy deposition

In most applications, a pyroelectric energy meter is quantitatively monitoring the laser pulse. We apply such a device (PE50, Ophir) for calibration and validation, too. The transferred energy is given simply by the difference of the detected energy before and after plasma breakdown. For this setup the location of the detector is found to be critical: Defocusing via thermal lensing of the plasma may lead to a partially more diverging beam behind the focus. Thus, in order to avoid measurement errors the detection system has to be placed near enough to the focal plane, but outside enough from plasma volume expanding. In practice, constant energy is found within a certain distance range. Applying this method to the PQL mentioned above, 12.1 ± 0.2 mJ is obtained in front of plasma and 8.1 ± 0.2 mJ behind plasma. Of course, these results do not provide any information about the temporal process of energy transfer. However, if pump current or pump duration of PQL increase, sequences of pulses are emitted with a constant pulse separation (~ 100 μ s). Applying the described method to the energy transfer of such pulse trains, only the overall energy before and after the breakdown can be detected. Even faster commercial energy detectors (Ophir, Gentec) do not resolve complex spatial-temporal energy distribution of individual pulses within the train. Insufficient time resolution may cause erroneous measurement, if the initial or transmitted energy is unequally distributed.

These arguments give reason for the development of a new method to investigate global energy deposition without such difficulties, a technique to distinguish temporal shape as well as quantity of energy transfer. High reproducibility and applicability to different PQL ignition systems are in demand. To demonstrate the applicability of the presented measurement technique to a complex temporal pulse profile, a laser is selected in this chapter which shows an apparent temporal double pulse structure due to high order laser modes.

The setup (Fig. 1a) consists of diffusors, a band pass filter (BP1064) transmitting the laser light and a fast pin-photodiode (SIR5-FC, Thorlabs) connected to a 4 GHz digital storage oscilloscope (DSO) (640Zi, LeCroy). For detection of the temporal shape of a laser pulse before the plasma, the beam irradiates the diffusors without lenses. Behind the plasma breakdown, a second appropriate lens collimates the beam, forming a Kepler-type telescope. Thermal lensing of hot plasma has to be considered again.

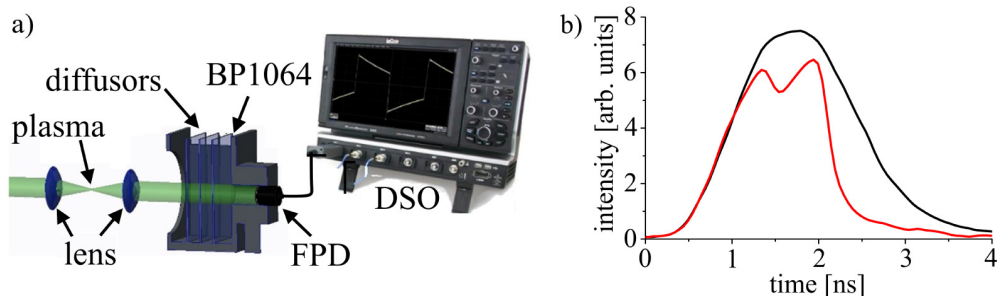


Fig. 1. (a): Setup for measuring the global energy deposition; (b): Spatially averaged temporal pulse profiles of a PQL pulse before plasma (black line) and after plasma (red line).

The results of these measurements are plotted in Fig. 1b. The black line corresponds to the measurement in front of plasma, the red one behind plasma. The energy transfer from laser to plasma is calculated to 32% by the ratio of the areas below the curves. This value is in good agreement with the one measured by a pyrometer. Beyond that, the described global method is able to detect the pulse shape and energy transfer of single pulses of a pulse train, even if

they are unequal. In this example, the pulse width of incoming laser shape is measured reproducibly to 1.7 ns FWHM (full width at half maximum). However, to explain the modified shape of the pulse transmitted, a more detailed view on its spatial pulse profiles is required.

2.2 Local energy deposition

In order to investigate such a non-uniform temporal and spatial energy distribution of a PQL, we developed a local method for measuring the energy transfer both temporally and spatially highly resolved. It is based on a modified version of the global method already depicted, aiming to resolve spatial energy distribution within the pulse profile. For this, a movable small pinhole of 250 μm in diameter placed in front of the diffusers scans the beam in Cartesian coordinates. The sketch in lower left-hand corner of Fig. 2 illustrates this approach.

The 3d-graphics present the results of a 16-step measurement of the red framed area before (a) and after (b) plasma breakdown. Temporal pulse shape is monitored at each position of spatial pulse profile. The spatial zero point corresponds with the center of the spatial pulse profile. The double pulse structure observed at this position before plasma generation (a) may arise from high order laser modes. Laterally, the double pulse merges into a temporal single pulse, occurring delayed to the first peak. For sensing such a delay, the oscilloscope is triggered externally by a vacuum photodiode (HS1, ITL), taking advantage of its large sensitive area related to pin devices.

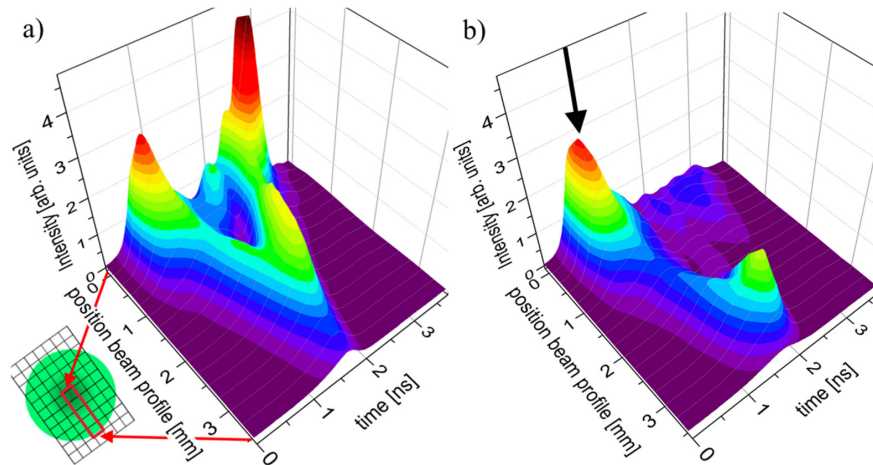


Fig. 2. Time-resolved energy distribution of beam profile before (a) and after plasma (b).

After plasma breakdown (Fig. 2 b), the second of these dual peaks is found to be removed totally. Furthermore, a strong decay appears in the spatial center of pulse (black arrow). Apparently, plasma breakdown takes place at this moment. Due to energy delay at the spatial position of 1-2 mm (Fig. 2), the energy deposition is high. For the outer edge (spatial position ~ 3 mm), deposition is reduced. An explanation could be the weak propagation of the plasma at ambient conditions with such a laser pulse.

Due to sequential x - y -scanning of the complete profile, the method is beneficial for inspection of more complex spatial pulse profiles, as they may appear in other pump geometries of PQLs [17,19].

3. Energy transfer of laser spark plugs

In PQL driven engine ignition systems (as spark plugs) the laser and its focusing unit are integrated into mounts, having optical access to the engine (Fig. 3). Thus, due to the sealed

setup, beam inspection as described in chapter 2 before the integrated focusing lens is inhibited.

However, due to improvement of the method (as follows) and by inserting a vacuum chamber preventing the pulse from plasma generation, global and local energy transfer of the five sealed laser spark plug prototypes (Table 1) can be analyzed quantitatively, too. Four of them are chosen with differences in pulse energy and temporal pulse width. The fifth spark plug has almost identical properties with one of the others and serves as a reference in regard to the measurement method and the design of the laser. The temporal shape of all five lasers is without any double pulses like observed in chapter 2.



Fig. 3. Prototype of a miniaturized passively Q-switched end-pumped laser spark plug produced by Robert Bosch GmbH.

Table 1. Examined laser spark plugs

Energy	FWHM	Focus Position
12.3 mJ	2.4 ns	11 mm
12.1 mJ	2.4 ns	11 mm
8.4 mJ	3.4 ns	10 mm
9.2 mJ	0.9 ns	10 mm
8.1 mJ	0.9 ns	12 mm

3.1 Experimental setup

To preserve plasma generation the sealed PQL with integrated focusing lens is docked to a vacuum pressure chamber. The chamber is optically accessible, temperature controlled and can be filled with different gas mixtures. The beam focus of the sealed spark plugs is centrally located within the chamber. While no plasma generation happens in the vacuum, the laser pulse leaves the chamber unaffectedly through the window on the opposite side. A suited lens again collimates the beam, forming a Keplerian telescope together with the focusing lens of the sealed spark plug. The collimated light is then sent to a filter box for spatial filters. A second lens downsizes the transmitted laser beam, approximately reaching its origin diameter. The subsequent detection unit is similar to the one described in chapter 2. The signal of a fast photodiode with a rise time < 35ps (UPD-35-IR2-P, Alphalas) feeds an 8 GHz DSO (Wavemaster 8Zi-A, LeCroy).

For investigation of pulse energy in time and space before plasma breakdown, an ordinary vacuum pump removes the gas from the chamber. So, plasma breakdown is prevented. The pulse is transmitted unaffectedly and is assumed to be identical to the incoming one (see chapter 2). All measurements were performed with breakdown in air and at room temperature.

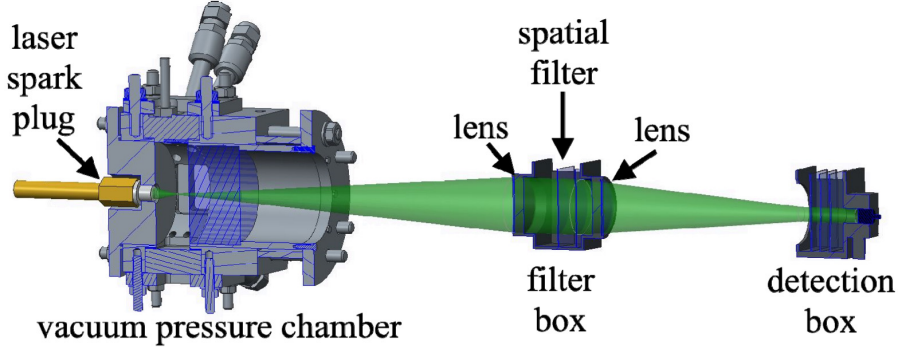


Fig. 4. Setup for measuring the global and local energy deposition of laser spark plugs.

3.2 Global energy deposition

To analyze the global energy deposition, the chamber was evacuated and no spatial filters are applied. The higher the local power density of a laser pulse is, the lower gas density is needed for suppressing a plasma breakdown. For investigation of the five sealed prototypes, a pressure below 0.1 bar appears to be sufficient to prevent a breakdown.

The area below these temporal emission curves is proportional to the amount of energy emitted from the sealed devices. So each detected intensity profile of the laser can be transferred into its power course (Fig. 5). It is evident that the two plugs with 12.3 mJ and 12.1 mJ single pulse energy show similar temporal profiles with identical pulse width of 2.4 ns FWHM. A third plug with 8.4 mJ pulse energy and 3.4 ns FWHM has a similar initial pulse rise. Two further plugs with shorter pulse widths (FWHM = 0.9 ns) slightly differ in their rise time. In Table 1 a summary of all values is given. With respect to the inaccessible sealed PQLs, the position of focus is defined here as the distance between plug exit window and location of the plasma breakdown.

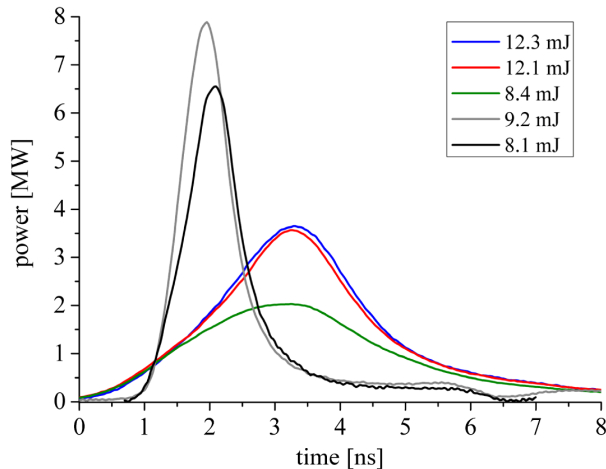


Fig. 5. Global temporal pulse profiles of five different spark plugs in vacuum.

If the pressure in the chamber increases, plasma breakdown takes place at the focus position. With increasing pressure, more energy is transferred from laser to plasma. Consequently, the detection system records less energy. To illustrate the impact of rising pressure, Fig. 6 shows the global temporal pulse profiles of the 12.3 mJ plug at different pressure levels. It is evident that the rising slopes are similar until an abrupt drop appears at

the moment of plasma breakdown. The temporal delay approaching between maximum power and breakdown in the curve at 0.7 bar is addressed in chapter 3.4.

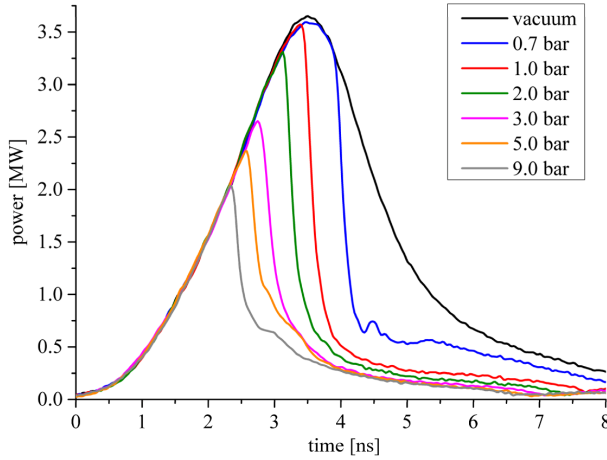


Fig. 6. Global temporal pulse profiles of plug 12.3 mJ for different pressure levels.

By integrating the area below the depicted shapes, the relative transferred energy for each pressure level can be calculated. Figure 7 summarizes the results of all investigated plugs. Error bars are plotted for the 9.2 mJ plug to illustrate the accuracy of the results presented. Errors may occur from little fluctuations of the laser system. Nevertheless, the overall reproducibility of the presented method is very high.

The energy transfer of the plugs differs most below 1 bar pressure. Plugs with a short power rise time and high maximum power transfer energy to plasma more efficiently. Relative energy transfer raises with pressure for all plugs, but this behavior saturates at more than 3 bar. All curves converge asymptotically to levels between 65% and 75%. At maximum pressure of 9 bar, the plug with 8.4 mJ transfers a little less, the plug with 9.2 mJ with a short power rise a bit more energy than the other plugs. A clear correlation between relative energy transfer for increased pressure and pulse width, power rise time or pulse energy cannot be found.

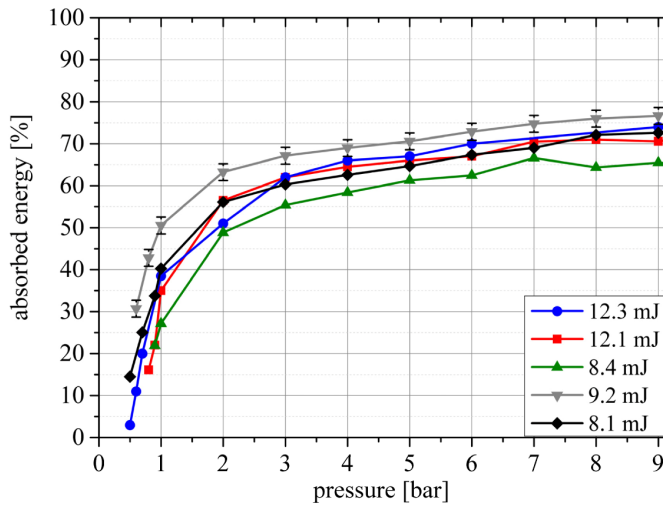


Fig. 7. Deposited energy of five different laser spark plugs at various pressure levels.

3.3 Local energy deposition

The spatially resolved energy deposition of the spark plugs is analyzed similarly to chapter 2. To increase the significance and to simplify the measurement method simultaneously, advantage of the radially symmetric spatial pulse profile is taken. Now the pulse is not resolved by rasterizing in spatial steps but in ring areas. This is performed by spatial ring filters inside the filter box (Fig. 4). So certain parts of the collimated light beam can be blocked. Our investigations show that global temporal pulse profiles can be calculated by summation of pulse profiles from measurements of different complementary ring area filters. Due to this finding, a subtraction of temporal profiles measured with one bigger and one smaller circular filter is found to be in good correlation with the one done by an appropriate ring area filter. Circular filters are more precise to build and easier to handle than ring area filters. Seven of such circular filters are employed in order to investigate on local energy transfer of the plugs. Subtracting the detected curves results in eight temporal pulse profiles. To consider temporal delays between the curves, the DSO was triggered by a vacuum photodiode again.

Figure 8 shows such a temporal pulse profile of the 12.3 mJ plug before breakdown (colored graphs). In the legend each color is assigned to a ring area. Additionally to the local measurements, the global temporal profile is detected without spatial filters (black line). The addition of all local curves is drawn by a dashed line. The good agreement demonstrates that the global pulse profile can be detected directly by measuring without any spatial filtering as well as indirectly by summation of local pulse profiles detected at individual spatial parts. The more central the local temporal profiles are located in the spatial pulse profile, the earlier the curves rise and the less the measured power is. Thus most energy of the pulse (area below the curves) is located in the outer areas of the spatial pulse profile, which occur with an obvious temporal delay to the central part of the laser.

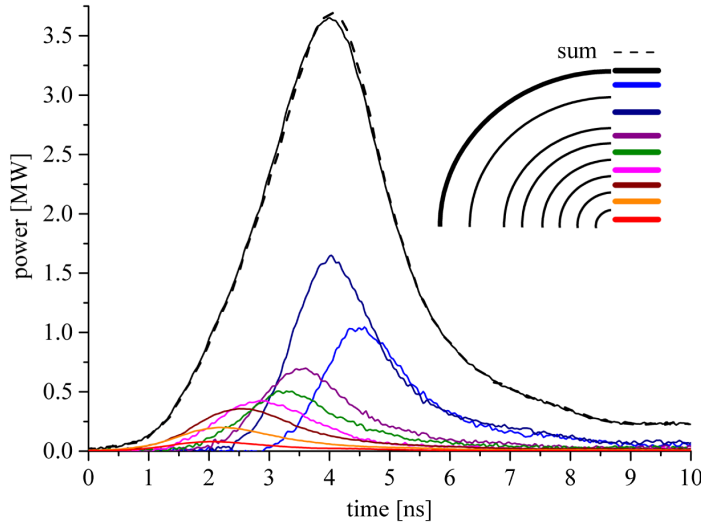


Fig. 8. Global (black) and local (colored) temporal pulse profiles of the 12.3 mJ plug in vacuum and sum of all local profiles (dashed black line).

If the pressure in the chamber increases, a plasma breakdown happens and an energy transfer from laser to plasma takes place. In Fig. 9, the profiles in time and space for 9 bar pressure are drawn with solid lines. For clarity, only every other value is depicted. The dashed line represents the results without breakdown in Fig. 8. The good match for the initial power gain demonstrates again the high reproducibility of this technique.

The breakdown takes place at a time before the outer ring area(s) arrive(s) at the focus position. The plasma induced before by the inner parts of the spatial pulse profile is optically dense and can absorb effectively the later arriving laser radiation. Within the measurement accuracy (< 100 ps), the plasma breakdown takes place simultaneously in all spatial parts of the pulse profile.

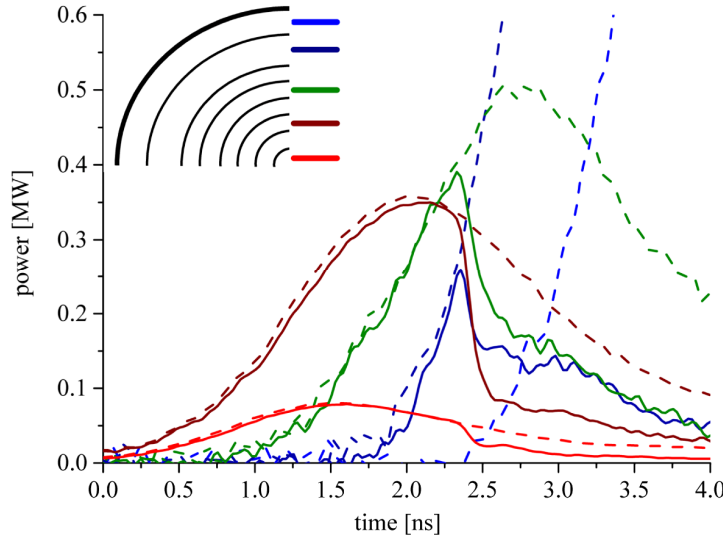


Fig. 9. Temporal pulse profiles for different ring areas of the spatial profile of plug 12.3 mJ.
Vacuum conditions are plotted in dashed lines, solid lines indicate situation at 9 bar pressure.

3.4 Breakdown process

In the presented work laser induced sparks are created by non-resonant breakdown. Different processes are involved here. Initial electrons have to be produced first. Multiphoton ionization takes place only at short wavelengths or at very low pressure [25,26]. In practical combustion processes, laser radiation is absorbed by impurities, which lead to high local temperatures and finally to free electrons [27,28]. These free electrons gain kinetic energy by absorbing more photons via the inverse bremsstrahlung process. The high energetic electrons ionize surrounding molecules by collision and new electrons are generated. This leads to an electron avalanche and to the breakdown of the gas [2,3,25,26,29].

Phuoc [1] and Bradley et al. [12] reported breakdown thresholds at atmospheric pressure of $1.65 \cdot 10^{16} \text{ W/m}^2$ and $2 \cdot 10^{15} \text{ W/m}^2$, respectively. They define the breakdown level as the energy threshold for more than 50% or 100% probability of breakdown. Chen et al. [30] define the breakdown threshold like Phuoc. They point out that if the maximum laser pulse intensity is higher than the breakdown threshold, all the energy above this threshold is absorbed by the plasma. This fact is applied to our measurements to determine an analogous defined breakdown threshold. Hence, the breakdown threshold is the global laser power density at which breakdown occurs and is indicated by a sharp falling edge in the temporal pulse profile. The breakdown thresholds measured for each spark plug at different pressures are in accordance with the investigations of Phuoc [1] and Bradley et al. [12]. These breakdown thresholds are considered with regard to global pulse profiles. However, local power density in the pulse profile can be significantly higher. For example, the breakdown threshold as defined above for the 12.3 mJ plug is found to be $3.1 \cdot 10^{15} \text{ W/m}^2$ at atmospheric pressure and $1.8 \cdot 10^{15} \text{ W/m}^2$ at 9 bar. In contrast, the local power density reaches a value of $2.6 \cdot 10^{16} \text{ W/m}^2$ for all pressure levels. As mentioned before the laser pulse releases spatially at

different times. This indicates the necessity to consider both temporally and spatially resolved pulse profiles for investigating the breakdown process.

To discuss this phenomenon for the investigated PQL spark plugs in detail, the local temporal pulse profile of the 12.3 mJ plug (Fig. 9) at 9 bar pressure is converted into dependencies of power density in focus, assuming the beam waist to be 19 μm . These results are plotted in Fig. 10. Spatially central parts of beam provide highest power density. The smallest circular spatial filter is chosen such that even smaller size does not increase power density significantly.

An apparent delay is found between maximum power density and plasma breakdown. Taking a closer look and considering a spatial distribution of pulse energy and power density, such a delay exists even at higher pressures. It is already indicated in the global energy transfer measurements at 0.7 bar (Fig. 6). At laser-induced breakdown with nanosecond pulses, such a delay can occur due to the necessary time for heating the electrons by the laser pulse above the threshold ionization energy of the molecules [14]. However, Fig. 10 shows again that plasma breakdown happens simultaneously in all spatial parts of pulse.

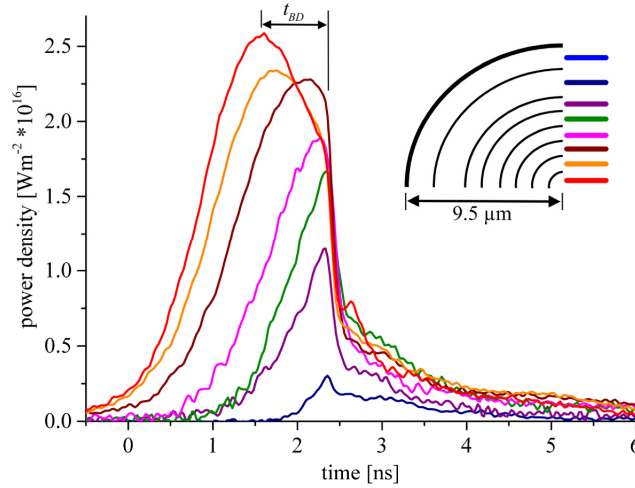


Fig. 10. Temporal power density of the spatially separated pulse profile of the 12.3 mJ plug at 9 bar pressure.

For detailed investigation, a breakdown delay t_{BD} is defined as a delay between maximum power density and plasma breakdown. This characteristic was determined for all five plugs at different chamber pressures and is summarized in Fig. 11. For each plug the delay decreases with increasing pressure, approaching asymptotically a limit. The delay of the three plugs with longer pulse widths and similar incident power rise (Fig. 5) is much longer than the delays of the plugs with short pulses. For a pressure of 1 bar or below, t_{BD} is smaller if the pulse width is smaller and the power rises more sharply. Above 2 bar t_{BD} of the three plugs with longer pulses are similar within the measurement accuracy (< 100ps). That could be expected because breakdown takes place within a period where power rise of the three plugs is similar (Fig. 5). Although this happens for shorter pulses in an earlier stage, t_{BD} of these plugs approach for increasing pressure. However, for a pressure above 5 bar a further decrease is not resolvable any more. The expected temporal change is smaller than the resolution of photodiode and oscilloscope applied.

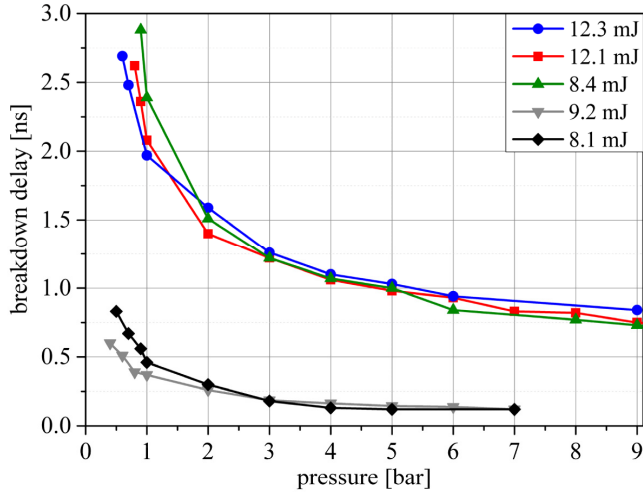


Fig. 11. Breakdown delay of five different laser spark plugs at different pressure levels.

The relative energy transfer of all investigated plugs is similar at higher pressures (Fig. 7). To link this results with the differences in breakdown delays, the local temporal profiles have to be regarded again (Fig. 8, 9). In chapter 3.2 it is shown as an example for the 12.3 mJ plug that the largest part of the pulse energy is located in the outer ring areas of the spatial pulse profile. While increasing pressure, most of this energy reaches the focus after the breakdown and is absorbed by the optical dense plasma. Integration of each local curves results in a quantitative energy distribution of the spatial pulse areas. To illustrate how much energy from each ring area at which pressure is transmitted, Fig. 12 shows the distribution of the transmitted energy of each ring area. To compare the distribution of plugs with different pulse widths, the results of the 12.3 mJ plug (Fig. 12 a) and the 9.2 mJ plug (Fig. 12 b) are given. As shown in Fig. 7, the total transmitted energy decreases with increasing pressure. Figure 12 demonstrates that from the center of the spatial pulse profiles hardly any energy is transferred from the pulse to the plasma. As discussed above, Fig. 12 a) shows again that above 3 bar pressure, nearly the total energy of the outer ring area is transferred to the plasma. In case of plugs with shorter pulse width (Fig. 12 b) there is no total energy transfer of any ring area.

The shorter the global pulse width and the power rise time is, the earlier the saturable absorber may allow laser light passing through the outer spatial pulse areas of the laser. Thus, the temporal delay decreases between the spatial central measured temporal pulse profile (with high power density and lower energy) and the spatial outer measured temporal pulse profile (with lower power density but much energy). For the investigated lasers with 0.9 ns pulse width, proportionally more energy of the energy-rich outer areas of the spatial pulse profiles passes the focus before breakdown. The plotted energy distribution at higher pressure illustrates this result (Fig. 12 b).

Thus, there are two competing effects having a positive impact on the energy transfer: If the pulse width of a PQL is appropriate, the phase of plasma building can be temporally separated from the phase of energy transfer. In case of laser pulses with faster power rise time and higher maximum power, an advantageous reduction of the plasma breakdown delay has been found, but the discussed separation gets lost.

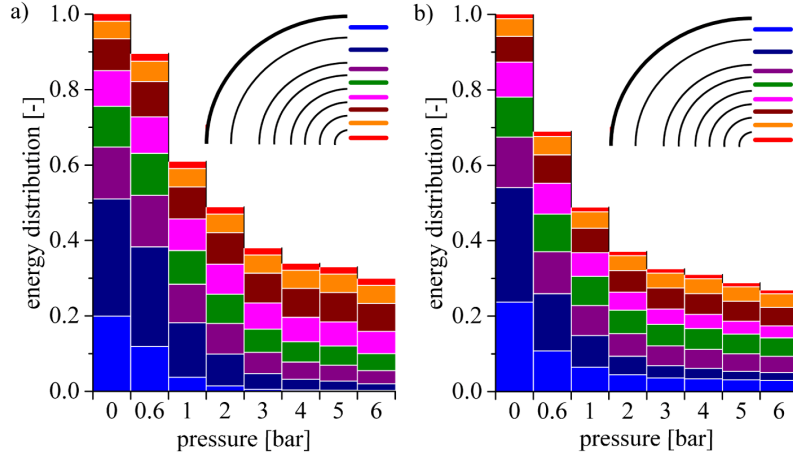


Fig. 12. Spatially separated energy distribution within the transmitted laser pulse profile of 12.3 mJ plug (a) and 9.2 mJ plug (b) at different pressure.

4. Conclusion

A new technique for temporally highly resolved characterization of the energy transfer from PQL pulses to plasma is introduced. It distinguishes between quantitative time-resolved measurements of global energy deposition and time-resolved measurements of local energy deposition, considering the energy distribution within the beam profile. Applied to different prototypes of laser spark plugs, the global investigations provide quantitative information about global pulse shape, pulse width and relative energy transfer into plasma. The results show that energy transfer of PQL pulses increases with shorter pulse width and fast power rise below 1 bar in air. At more than 3 bar the relative energy transfer of all investigated plugs converges asymptotically to levels between 65% and 75%. A clear correlation between relative energy transfer and pulse width, power rise time or pulse energy cannot be found at increased pressures. By local measurements, the influence of complex spatial-temporal pulse profiles on the process of plasma breakdown is demonstrated. The generation of plasma was found to be not only depending on a maximum power density in the laser focus. A temporal delay exists between the moment of maximum power density and the plasma breakdown. This delay decreases with increasing pressure and depends on rise time of the global temporal pulse profile. Moreover, for pulses with sufficient global pulse width, the delay causes an advantageous separation of a plasma-building phase from a phase of energy transfer. In case of laser pulses with faster power rise time and higher maximum power, an advantageous reduction of the plasma breakdown delay has been found but the separation of a plasma building phase from a phase of energy transfer disappears for pulses with a short pulse width. Thus, all investigated laser spark plugs have a similar energy transfer relative to their pulse energy at increased pressures.

The presented measurement technique enables new studies on optimization of laser impulse design for ignition processes and other applications of miniaturized passively Q-switched lasers.

Acknowledgments

The authors are grateful for the financial support of the German Research Foundation (DFG) under grant no. BR 1713/13-1. Furthermore, the authors thank the Robert Bosch GmbH for the numerous helpful discussions and prototypes of PQL-spark plugs granted as a loan. This publication was funded by the University of Bayreuth in the funding programme Open Access Publishing